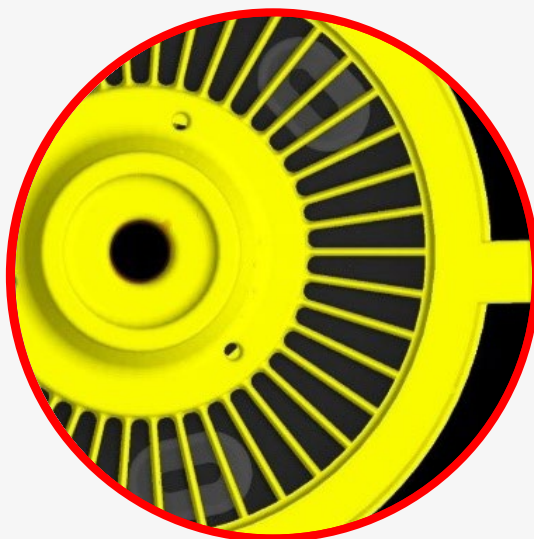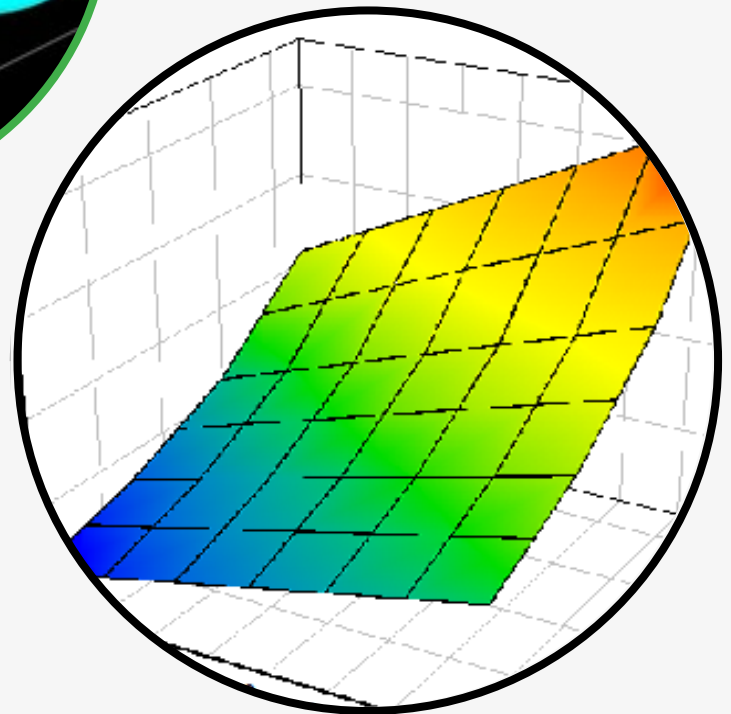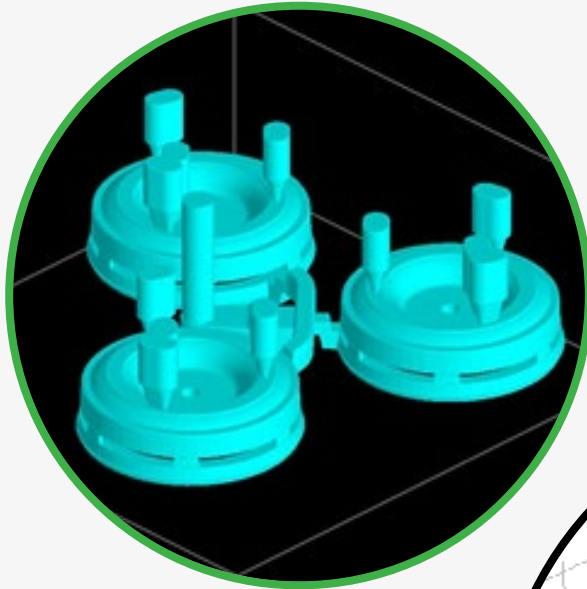# JOURNAL OF CASTING
& MATERIALS ENGINEERING

AGH UNIVERSITY OF SCIENCE AND TECHNOLOGY
FACULTY OF FOUNDRY ENGINEERING

JCME

Contents

Optimization of a Gating System by Means of Simulation Software to Eliminate Cold Shut Defects in Casting

Vladimír Šabík[a*], **Peter Futáš**[a] , **Alena Pribulová**[a] , **Petra Delimanová**[a]

[a]Technical University of Kosice, Faculty of Materials, Metallurgy and Recycling, Letná 9 Košice, Slovakia
*e-mail: vladimir.sabik@tuke.sk

Abstract

The current trend in foundries is to achieve the production of high quality and competitive cast components. The innovation and optimization of current processes is a necessary element to achieve this goal. With the help of numerical simulations, it is possible to replace financially demanding and time-consuming experiments in real conditions with simulations that can reliably represent foundry process using computer technology. By a detailed analysis of the simulation results, we can predict various risks that could negatively affect the production process. This article monitors the influence of changes in the design of the gating system on the surface quality of a clutch wheel casting made of ductile iron, in the production of which two models of the gating system for casting were constructed in CAD software. Verification of gating systems was performed using the simulation software NovaFlow & Solid. The aim of the design change of the gating system is to reduce the amount of liquid metal used per casting, which can have a significant economic impact on industrial production. For this purpose, several simulations of the gating system of the casting were performed, while 2 which are the most representative for the mentioned problem were selected for the needs of the article. The main task of the simulation was to set the cellular network and conditions as close as possible to the reality of casting and the subsequent design and modification of the gating system.

Keywords:

numerical simulations, gating system, clutch wheel, cold shut

1. INTRODUCTION

In the production of each casting component, an effort is made to achieve the required quality at the lowest possible cost. Through simulation software it is possible to simulate processes with a relatively high degree of accuracy during the casting of liquid metal and the solidification of the casting. In the production of quality castings, the simulation of filling and solidification of castings is an integral part of production quality. Computer simulation of casting processes is a highly effective tool for optimizing processes and events that take place during the filling of the mould cavity and casting cooling. In the pre-production stage, flaws in castings such as shrinkages and micro porosity can be prevented by the simulation of filling and solidification. Adjustments to the gating and feeder systems, along with technological adjustment of casting and casting parameters by means of a computer simulation, can help to prevent such flaws [1–4].

Numerical simulations are a tool that can be used to evaluate foundry processes by means of computer technology and to analyze various risks that might adversely affect the production process. By using software and setting the input data correctly, it is possible to favorably influence and even eliminate the trial and error method which has long been used in some foundries. By direct optimization, it is possible to not only reduce the input costs to produce a given series of castings but also the costs associated with determining the cause of the defect. The digitizing of the production process in the foundry should consist of two main steps [5]:

- execution of a 3D model in CAD system (Catia, SolidWorks, Autodesk 360),
- implementation of foundry process simulations in a simulation software (Magmasoft, Novaflow, ProCast).

Numerical modeling in the foundry industry is based on the use of empirical and semi-empirical physical and numerical models [6]. By using simulation software, which already includes a numerical model describing the processes taking place in the foundry process, we obtain sophisticated solutions of complex processes, which can be subsequently analyzed. Commercially available software packages that are currently available for foundry needs are affordable and can replace demanding operational experiments [7].

The casting simulation software consists of three modules:

- solidification simulations,
- flow simulations,
- combined simulation.

The solidification simulation can be used to detect the location of hot spots, to design and modify gating system. The flow simulation can help us to visualize melt velocity during mold filling, filling time and solidification time, which helps to locate melt flow disturbances such as imperfect melt flow, gating system malfunction, etc. [8, 9].

2. EXPERIMENTAL PART

The 3D model of the casting (Fig. 1) with many rib parts was created in CAD software SolidWorks. The computer simulations were realized by the software NovaFlow & Solid.

Fig. 1. 3D model of casting

The EN-GJS-500 alloy was the model material. The melt flow was 11 kg·s^{-1}, the casting type was gravity casting. The melt was poured into the mold made of uniform bentonite mixture. After creating individual variants of the gating system in the CAD software SolidWorks, it is necessary to import the 3D model into the simulation program NovaFlow & Solid, and configure the input parameters of the simulations so that they correspond as much as possible to real conditions.

Table 1 shows the summary of simulation inputs.

Table 1
Summary of simulation inputs

Casting type	Gravity casting
Alloy	EN-GJS-500
Flow	11 kg·s^{-1}
Casting temperature	1410°C

In Figure 2, the entire system is imported into a simulation program. A cell in a model is an element in which a program can evaluate individual processes (the more cells, more accurate the results). As the number of cells increases, the computation time of the simulation increases, too.
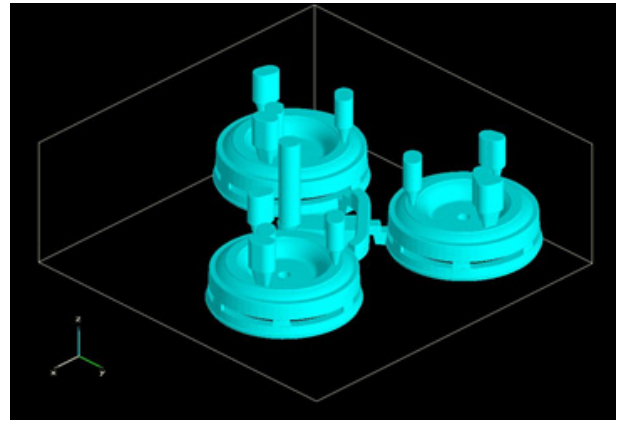
Fig. 2. The cellular network of the model imported in the simulation software NovaFlow & Solid

3. SIMULATIONS

During the casting production, there was insufficient flow of molten metal into the ribbed parts. Figure 3 shows a 3D model of the original implemented design of the gating system with 3 castings.

a)

b)
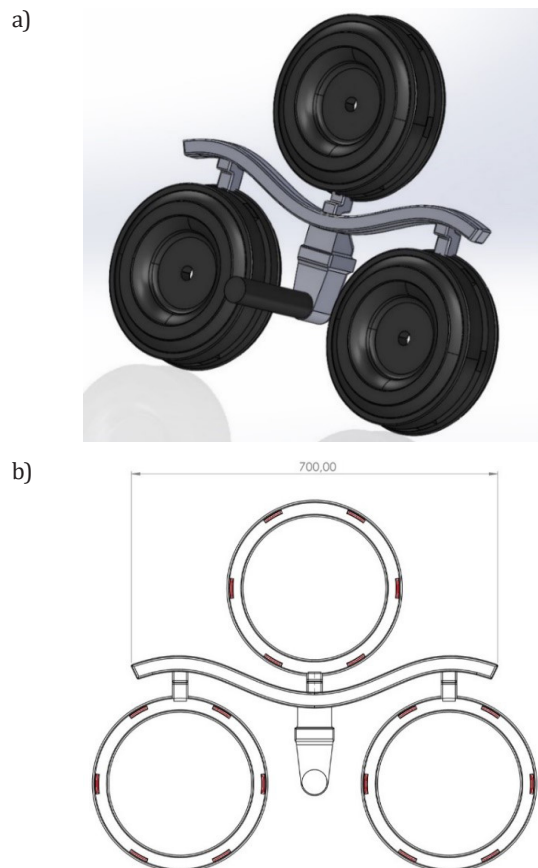
Fig. 3. Gating system with 3 castings: a) 3D model; b) original design

After the observed simulation of the original design (Fig. 4), it was found that at the value of 49% of the mold filling, the melt was flowing from outside of the ribs of the casting towards central part, which comes into contact with the melt, which was flowing in the opposite direction. The contact area in these places is too large due to the flowing melt volume through this cross section.

Fig. 4. The original design of the 49% filled form – detail of risk areas

In Figure 4, we can see red (high proportion of liquid phase) and in some places gray color (solidified metal), which corresponds to the real occurrence of defects in the casting. Therefore, this point was chosen for investigation. The form reaches 49% filling in the time of 3.460 s. These factors can cause the defect known as cold-shut. Cold-shuts are visible on the casting as missing part of the casting without fracture.

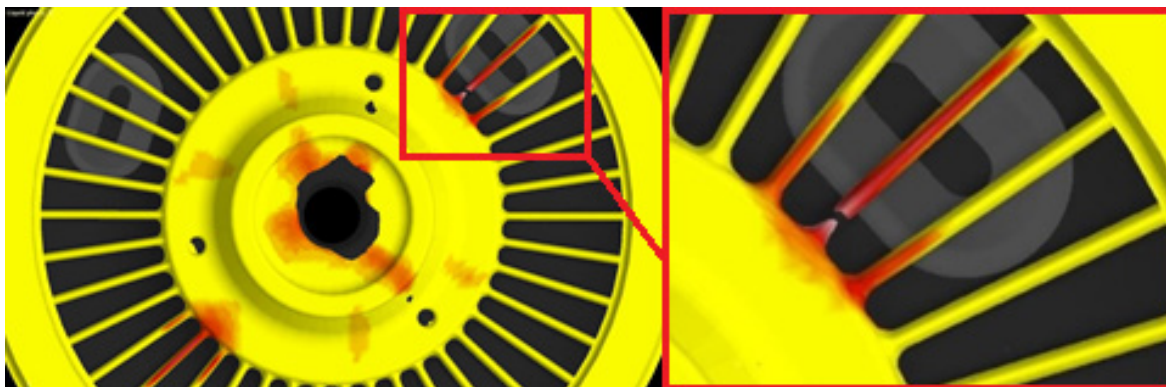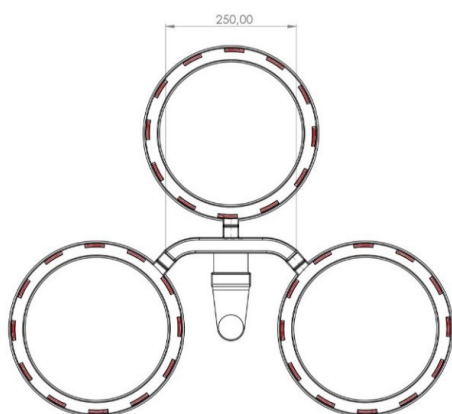Figure 5 shows the improved gating system of the casting.

Fig. 5. Improved gating system

Figure 6 shows the proportion of liquid phase only. This indicates directional solidification and the casting should solidify without defects. At the same time, the form reaches the 49 filling in the time 3.168 s after changing the gating system design.
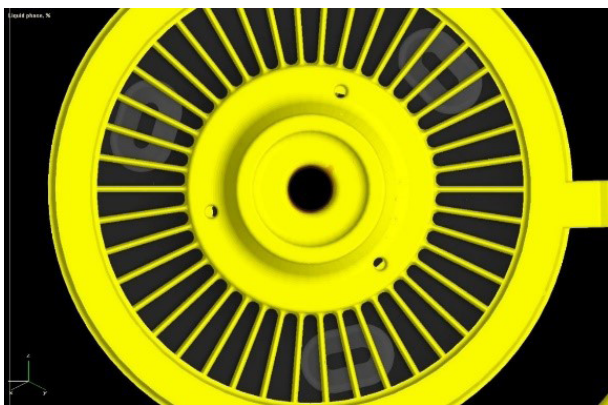

Fig. 6. The improved gating system of the 49% filled mold – the detail of risk areas

4. CONCLUSION

Results are based on mold filling simulation as well as solidification simulation. Those methods were used to reveal the possible cause of the casting defect. The construction modification of the gating system eliminated the cause of the casting defect by means of the faster distribution of molten metal into risk areas. The filling time of the mold in the case of the original design of the gating system was 3.460 s. In the case of the improved gating system, the filling time was 3.168 s, and this difference in times led to the elimination of the occurrence of the defect. Improvement of the gating system design would significantly suppress the occurrence of the defect and represent economic savings in terms of cast iron consumption.

We can see the important difference between the weight of the original design of the gating system and the variant with the improved gating system of up to 4 kg. This weight difference represents 4 of cast iron per year for mass production. The costs associated with the casting of test specimens would help to achieve the elimination of defects and would significantly reduce failures in casting.

Acknowledgements

REFERENCES

[1] Olofsson J., Salomonsson K. & Svensson I.L. (2015). Modelling and simulations of ductile iron solidification-induced variations in mechanical behaviour on component and microstructural level. *IOP Conference Series: Materials Science and Engineering,* 84, 12026. Doi: https://doi.org/10.1088/1757-899X/84/1/012026.

[2] Sulamet-Ariobimo R.D., Soedarsono J.W. & Suharno B. (2015). Cooling Rate Analysis of Thin Wall Ductile Iron Using Microstructure Examination and Computer Simulation. *Applied Mechanical and Materials,* 752–753, 845–850. Doi: https://doi.org/10.4028/www.scientific.net/AMM.752-753.845.

[3] Bhatt H., Barot R., Bhatt K., Beravala H. & Shah J. (2014). Design Optimization of Feeding System and Solidification Simulation for Cast Iron. In: Procedia Technology. 2nd International Conference on Innovations in Automation and Mechatronics Engineering, ICIAME 2014, Gujarat, India, 7–8 March, 14, 357–364. Retrieved from https://www.sciencedirect.com/science/article/pii/S221-2017314000826.

[4] Futáš P., Pribulová A., Fedorko G., Molnár V., Junáková A. & Laskovský V. (2019). Failure analysis of railway brake disc with the use of casting process simulation. *Engineerign Failure Analysis*, 95, 226–238. Doi: https://doi.org/10.1016/j.engfailanal.2018.09.005.

[5] Jolly M. (2002). Casting simulation – How well do reality and virtual casting match? State of the art review. *International Journal of Cast Metals Research,* 14(5), 303–313. Doi: https://doi.org/10.1080/13640461.2002.11819448.

[6] Novacast (2018). *Release of NovaFlow&Solid 6.4.* Retrieved from https://www.novacast.se/news/release-of-novaflowsolid-6-4/ (accessed 1.02.2021).

[7] *MAGMASOFT® 5.4 – Autonomous Engineering.* Retrieved from https://www.magmasoft.co.in/export/shared/.galleries/pdfs_publications/2018_pm_en_magmasoft_rel_5_4.pdf (accessed 5.02.2021).

[8] Zexuan W., Tao H., Yong Y. & Yan L. (2015). Application and development of numerical simulation technology in Casting. *International Journal of Research in Engineering and Science (IJRES)*, 3(2), 23–28. Retrieved from https://www.academia.edu/12390402/Application_and_development_of_numerical_simulation_technology_in_Casting?sm=b (accessed 26.02.2021).

[9] Ha J., Cleary P., Alguine V. & Nguyen T. (1999). Simulation of die filling in gravity die casting using SPH and MAGMAsoft. In: Second International Conference on CFD in the Minerals and Process Industries, CSIRO, Melbourne, Australia, 6–8 December, 423–428. Retrieved from http://www.cfd.com.au/cfd_conf99/papers/045HA.PDF (accessed 5.02.2021).

Optimization of Blast Furnace Throughput Based on Hearth Refractory Lining and Shell Thickness

Chinwuba Victor Ossia[a]*⊙**, Shedrack Mathew Uzoma**[a]

[a]Department of Mechanical Engineering, University of Port Harcourt, Port Harcourt, Nigeria
e-mail: chinwuba.ossia@uniport.edu.ng

Abstract

Computational analyses were performed to optimize the furnace throughput, steel shell and lining thickness of a blast furnace. The computations were done for measured parameters within the hearth region as this is the vital zone of the furnace with high temperature fluctuations, molten iron, and slag production. The lining materials were namely 62% high alumina (A), carbon composite (B), silicon carbide (C) and graphite bricks (D) with thermal conductivities 2, 12, 120 and 135 W/(m·K), respectively. It was observed that by varying the refractory lining thickness from 0.2–0.35 m, and furnace inside temperatures from 1873–2073 K, certain optimal conditions could be specified for the furnace under consideration. Silicon carbide and graphite brick linings which have higher thermal conductivities, melting points, good chemical and mechanical wear resistance were observed to be the best hearth lining materials. Due to the high thermal conductivities of these two materials, the hot face temperature levels of the lining materials would be lowered. Amongst the four lining materials employed, silicon carbide and graphite bricks when used with lining cooling systems could optimize the blast furnace for better performance, production, and longer campaigns.

Keywords:

1. INTRODUCTION

1.1. Background

The blast furnace is the focus of any integrated steel plant. Blast furnaces are used to reduce iron ore (say, hematite Fe_2O_3) to wustite (FeO) to molten pig iron (Fe). The raw materials consist of iron ore, pellets and/or sinter, coke, and flux (limestone and quartzite). Reducing conditions on account of gaseous reductants carbon monoxide (CO) and carbon dioxide (CO_2) enable this transformation.

Some blast furnace (BF) parts like the hearth, bosh, belly, stack, blast furnace stoves may require different quality of refractories depending on the requisite operating conditions and available resources. This study concentrates on the hearth region as a crucial zone subjected to high temperatures, heat and chemical interactions and production of slag and molten iron through the tapholes.

Selection of appropriate refractory combination in the hearth depends on in-depth knowledge of iron-making system and the physical, mechanical and chemical properties of the proposed refractories [1].

An improper understanding of the above factors often leads to refractory failures like wear which subsequently become complex problems to solve. Refractory linings, whether of a blast furnace or any other metallurgical furnace, usually fail due to any number or combination of such factors like improper furnace temperature distribution, high thermal expansion coefficients, lack of resistance to acid and alkali attack, etc.

This study deals with optimizing the furnace throughput and proper selection of refractory material of right insulation thickness. Four types of refractory lining materials, namely 62% high alumina Al_2O_3, carbon composite, silicon carbide (SiC) and graphite bricks, are examined to investigate the most suitable lining for optimum furnace performance.

1.2. Blast Furnace

The blast furnace is a vertical counter-current heat exchanger and chemical reactor for producing hot molten metal known as pig iron. In counter current manner, the ascending gas (CO, CO_2, H_2 and N_2) flow and the permeable bed made up of iron ore, coke and flux descend. An illustration of the iron blast furnace is presented in Figure 1. The raw materials used in the process are coke, iron ore agglomerates of pellets or sinter and slag formers. Other materials that can be used are cold bonded briquettes, basic oxygen

furnace slag and scrap. Alternating layers of coke, iron burden and slag formers are charged at the top. The material descends due to gravity when the coke is continuously burned at the tuyere level and the slag and molten pig iron (Fe) is tapped from the hearth [2, 3].
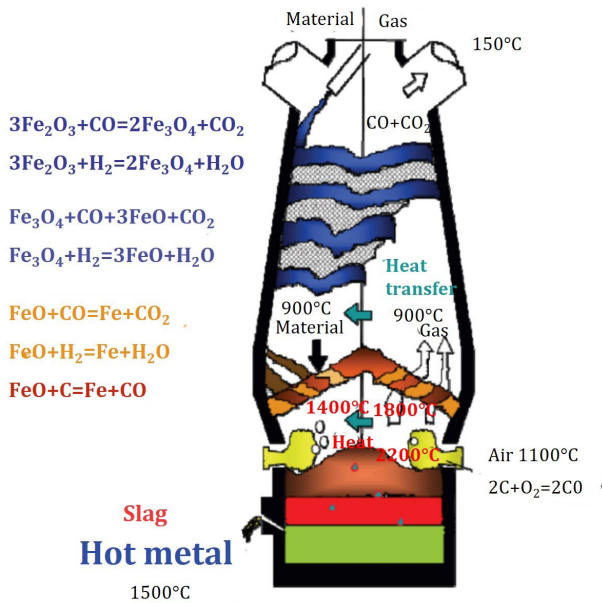

Fig. 1. Furnace cross section with the reactions at different heights [4]

The reduction of hematite to metallic iron occurs in different stages with different requirements on the reducing gas. To describe this, the carbon monoxide (CO) utilization factor, $\%\eta_{CO}$, is introduced as expressed in Equation (1):

$$\%\eta_{CO} = 100\% \cdot \frac{\%CO_2}{\%CO + \%CO_2} \qquad (1)$$

Table 1 shows the different utilization factors and CO/CO_2 ratios at equilibrium for the reduction of the iron oxides at 900°C. The reduction reactions given in Table 1 are called the indirect reduction of the iron oxides.

Table 1
CO utilization factors and CO/CO_2 ratios at equilibrium for iron oxides reduction at 900°C [1]

Reaction	CO/CO_2	$\%\eta CO$
$3Fe_2O_3 + CO = 2Fe_3O_4 + CO_2$	0	100
$Fe_3O_4 + CO = 3FeO + CO_2$	0.25	80
$FeO + CO = Fe + CO_2$	2.3	30

With reference to Table 1, it is observed that at 900°C the required ratio to successfully reduce wüstite, FeO, to metallic iron is 2.3 and the equilibrium reaction is as in Equation (2):

$$FeO + 3.3CO = Fe + CO_2 + 2.3CO \qquad (2)$$
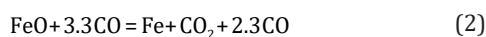
The counter-current outline of the process enables a gas rich in CO to come into contact with the wüstite FeO. The gas is then successively depleted in CO while ascending in the furnace, reducing the iron oxides. An ideal temperature profile with the associated chemical reactions is depicted in Figure 2.

No single refractory material will satisfy the physical, chemical, and metallurgical demand of a blast furnace's operational demand. This work is devised to seek the right type of refractory material lining thickness and optimal shell thickness in the hearth region of a blast furnace for optimal throughput delivery. Table 2 shows the distribution and type of refractory lining in the different sections / zones of a blast furnace.
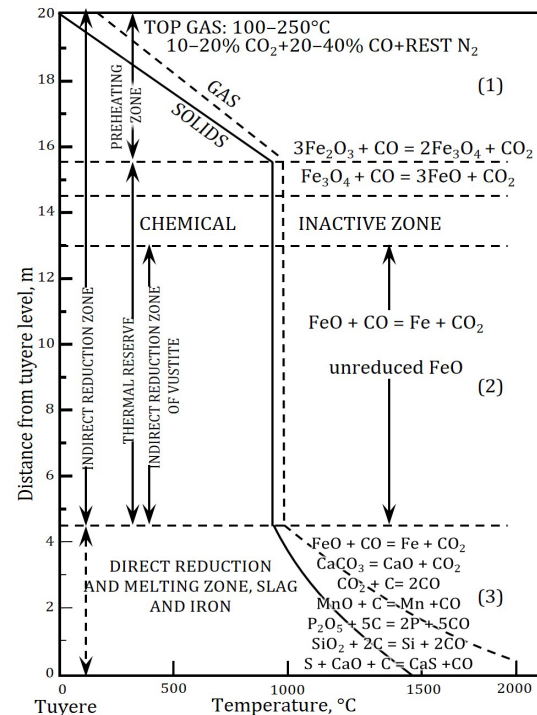
Fig. 2. Ideal temperature profile for the blast furnace represented as the height above tuyere level [1]

Table 2
Blast furnace refractory materials distribution

Area	Refractory nomenclature	Trend
Stack	39–42% Al_2O_3	super duty fireclay
Belly	39–42% Al_2O_3	corundum, SiC-Si3N4
Bosh	62% Al_2O_3, mullite	SiC-Si3N4
Tuyere	62% Al_2O_3, mullite	SiC self bonded, alumina-chrome (corundum)
Lower hearth	42–62% Al_2O_3, mullite, conventional carbon block	carbon/graphite block with super micro pores
Tap hole	fireclay tar bonded, high alumina / SiC tar bonded	fireclay tar bonded, high alumina / SiC tar bonded
Main trough	pitch / water bonded clay / grog / tar bonded ramming masses, castables	ultra low cement castables (ULCC), SiC / alumina mixes, gunning repairing technique
Tilting spout	high alumina / SiC ramming masses / low cement castables	high alumina / SiC / carbon / ULCC

1.3. Blast Furnace Temperature Zones and Hearth Arrangement

The blast furnace is comprised of different regions, namely: stack / shaft (19.0 m high), belly (2.5 m high), bosh (4.3 m high), hearth (6.2 m high) and the base region (4.8 m high) [5]. And the total blast furnace height under consideration is 28 m. From Figure 3, the tuyere region has the maximum temperature of 2100°C, while the hearth region showed 1500–1450°C, bosh region 1000–600°C, and while the shaft and belly region showed a temperature range of 600–200°C from the temperature contours in Figure 3.
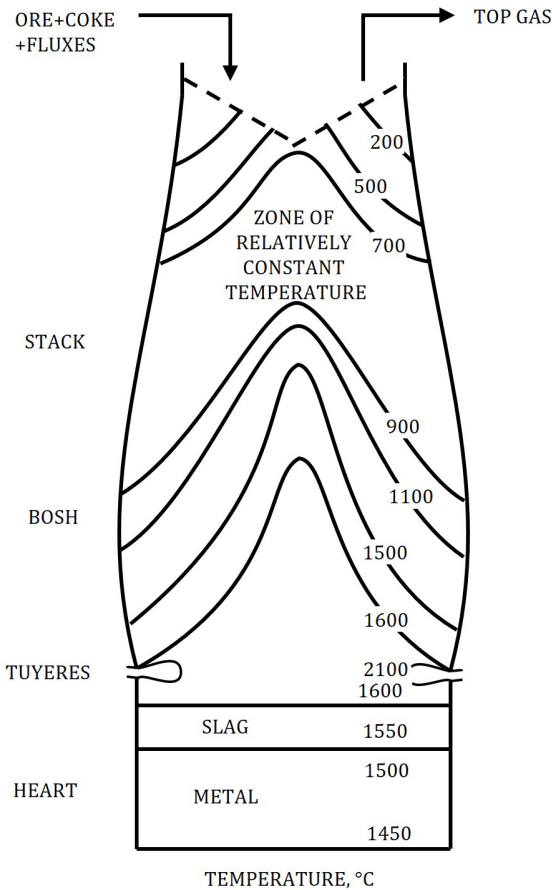

Fig. 3. Blast furnace temperature contours and the hearth region [6]

The furnace hearth is constructed by several refractory zones. The bottom part of Figure 4 (a) represents the dimension of the hearth under consideration. The taphole position is marked with the arrow line. The outside of the hearth is covered with a steel shell (a) in Figure 4. The wall and bottom are constructed from five types of refractory materials, each with its specific properties depending on what types of environment the region is exposed to. The wall (b) is made of any of the four lining materials under consideration – 62% high alumina, carbon composite, silicon carbide and graphite bricks. They have low to relatively high heat conductivities to keep the inner wall at a low temperature. The upper layer of the bottom (c) is a ceramic plate with the composition 23.5% SiO_2, 73.5% Al_2O_3 and some additives. It has a high resistance to mechanical wear to keep the bottom layer intact and avoid cracks. That is important to avoid

liquid iron penetrating and solidifying in the lower bottom layers (d), since this would have an impact on the heat flow. Between the steel shell and the bottom refractory is a layer of ramming paste (e). The blast furnace hearth is shown schematically in Figure 4. The taphole region in the hearth section shown in Figure 5 is made of a carbon refractory. It has very high heat conductivity to transport heat from the taphole during tapping and reduce the thermal stresses in the region.
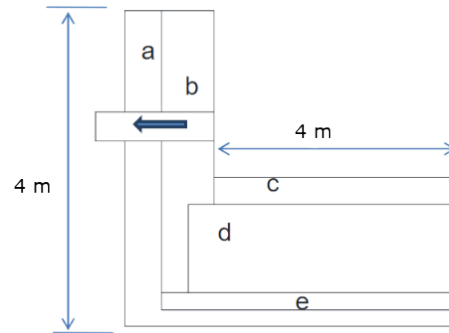
Fig. 4. Blast furnace hearth schematics – taphole is indicated by the thick arrow: a) steel shell; b) wall; c) upper layer of the bottom; d) the lower bottom layers; e) layer of ramming paste
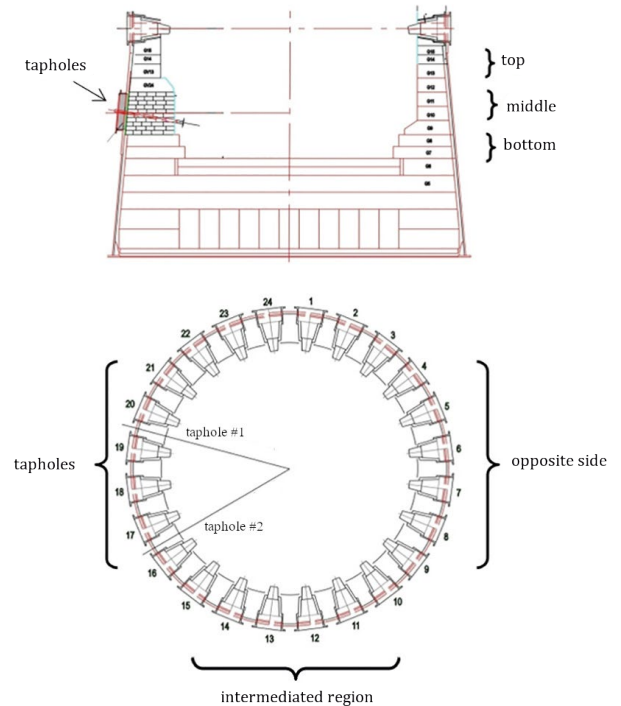
Fig. 5. Blast furnace hearth section [7]

The iron and steel industry is one of the key drivers of today's global economy. Efficient combustion and heat recuperation, recovery and conservation will improve pig iron production and this in turn will increase the economic and technological value of the furnace. Since the service life of the blast furnace depends largely on the state of the hearth lining and appropriate thickness, this research will aid the selection of better lining materials with superior properties and refractoriness.

2. MATERIAL AND METHOD

2.1. Hearth Lining Material Model

Over the years, considerable efforts have been put on finding ways to increase blast furnace productivity and extend the campaign length. The state of the hearth has been identified as the most important factor by many for a long furnace campaign length. This lower region of the furnace is exposed to liquid iron and slag at high temperatures that could be in direct contact with the lining, causing erosion and corrosion of the lining material. The most aggressive environment is found in the region closest to the taphole. It is exposed to thermal stresses and liquid iron and slag at high flow rates [8].

Increased productivity results in higher loads on the furnace which can potentially shorten the campaign length. To strive to optimize both these goals, it is important to carefully control the state of the hearth. Most blast furnaces are equipped with thermocouples, measuring lining temperatures. Monitoring the information provided by the thermocouples can give instant information about the lining temperature, but also enable studies of the temperature evaluation on both a long-term and short-term basis [4, 9].

Accordingly, the ability to control the state of the hearth and maintain a steady operation, are two key issues in blast furnace practice. It is therefore of importance to understand the process and be able to interpret its behavior. The research aims to study the heat flows through the blast furnace hearth lining, compare four lining materials and their properties by numerical modeling to ascertain the best material for optimal throughput delivery.

The optimization approach entails varying the lining thickness from 0.2 m to 0.35 m and comparisons with respect to the heat loads developed. Similarly, the furnace hearth temperatures will be varied from 2073 K to 2673 K to achieve various values of the conduction heat loads for optimum performance and productivities.

2.2. Model Formulation

The following valid assumptions are made in the process of formulating the combustion and heat load analysis for the blast furnace for optimization:

- the analysis is done on a single layer refractory lining area with a one-directional profile as a case study,
- heat flow density q in any location through the wall is constant,
- the models for the heat loads are derived at steady state; the implication being that no system parameter is time-dependent,
- the models developed subject to the fact that the furnace is very nearly cylindrical in structure. Based on the concept of the cylindrical coordinate system, the temperature at the center of the blast furnace is a maximum, but it is assumed to be the temperature at which solid iron changes to molten iron,

- the heat transfer at interfacial boundary zones is considered insignificant; hence the heat content of the different zones should be constant,
- optimization of the throughput and refractory lining will cover that of the steel shell, since the lining protects the shell from the high temperatures, chemical attacks and abrasive *materials* inside the furnace and most especially the high temperature hearth region; this simply means a suitable hearth lining material will enhance longevity of the steel shell in turn,
- the hearth space temperature is experimentally taken to be 1600°C (1873 K),
- effects and compositions of the liquid metal and slag in the hearth region are neglected.

Technically, heat transfer analysis is one of the major studies employed to understand and enhance the performance of many metallurgical furnaces. Schematically, the temperature distribution through the walls of the hearth is as shown in Figure 6.
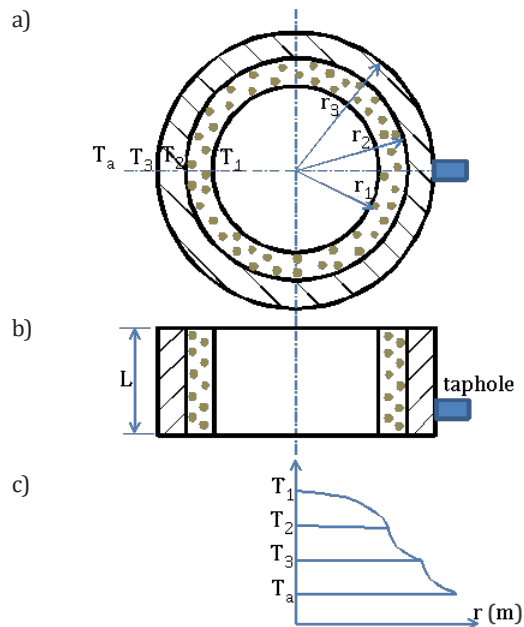
Fig. 6. Schematics and temperature profile of the hearth under study [3]: a) plan; b) elevation; c) temperature profile

Recall that Fourier's general law of heat conduction [10] can be expressed as Equation (3):

$$Q = \frac{-kA(T_2 - T_1)}{t} \tag{3}$$

where: t – thickness of the transfer medium (m).

The heat flux through the system – furnace workspace, lining and steel shell remains constant under steady state condition [10, 11]. Hence, the radial heat flux q_r is expressed as Equation (4):

$$q_r = -kA_r \frac{\partial T}{\partial r} \tag{4}$$

where: $A_r = 2\pi_{rL}$.

Substituting gives Equation (5):

$$q_r = -k2\pi rL \frac{\partial T}{\partial r} \qquad (5)$$

integrating both sides gives Equation (6):

$$\int q_r \left[\frac{\partial r}{r} \right] = \int -k2\pi L \partial T \qquad (6)$$

Inserting the limits of integration yields Equation (7):

$$\int_{r_1}^{r_2} q_r \left[\frac{\partial r}{r} \right] = -k \int_{T_1}^{T_2} 2\pi L \partial T \qquad (7)$$

This becomes Equation (8):

$$q_r ln \left[\frac{r_2}{r_1} \right] = k2\pi L(T_1 - T_2) \qquad (8)$$

The heat flux q_l through the inner lining with thermal conductivity k_l can be given by Equation (9):

$$q_l = \frac{2\pi k_l L(T_1 - T_2)}{ln \left[\dfrac{r_2}{r_1} \right]} \qquad (9)$$

Similarly, the heat flux through the steel shell with thermal conductivity k_{ss} can be given by Equation (10):

$$q_{ss} = \frac{2\pi k_{ss} L(T_2 - T_3)}{ln \left[\dfrac{r_3}{r_2} \right]} \qquad (10)$$

Similarly, the heat flux through the refractory material with thermal conductivity k_{rm} can be given by Equation (11):

$$q_{ss} = \frac{2\pi k_{rm} L(T_1 - T_2)}{ln \left[\dfrac{r_2}{r_1} \right]} \qquad (11)$$

Let the convective heat transfer coefficient of the melt and the surrounding air be h_m and h_a, respectively. Heat transfer by convection, q_{lm} to the internal surface of the furnace lining can be represented as Equation (12):

$$q_{lm} = -h_m 2\pi r_1 L(T_1 - T_m) \qquad (12)$$

The heat transfer rate from the surface of the steel shell to the surroundings by convection, q_{sa} is expressed as Equation (13):

$$q_{sa} = -h_a 2\pi r_2 L(T_a - T_3) \qquad (13)$$

Following similar arguments made by Briggs and Shedrack [3], and Gdula et al. [11], that under steady state conditions all conductive and convective heat flux must be equal, hence Equations (7)–(11) must be equal as in Equation (14):

$$q_r = \frac{2\pi k_l L(T_1 - T_2)}{ln \left[\dfrac{r_2}{r_1} \right]} = \frac{2\pi k_{ss} L(T_2 - T_3)}{ln \left[\dfrac{r_3}{r_2} \right]} =$$
$$= h_m 2\pi r_1 L(T_m - T_1) = h_a 2\pi r_2 L(T_3 - T_a) \qquad (14)$$

2.3. Furnace Input Data / Experimental Analysis

All the heat load analyses, refractory material thickness and shell thickness calculations and simulations in this study were performed through the simulation subroutine in the Appendix, while its results were used to prepare the charts (figures) using sigmaPlot software

The furnace refractory lining materials thermal conductivity data used are shown in Table 3, while Table 4 outlines the characteristics of the blast furnace used in this study to investigate the best refractory material properties with constant and varied furnace temperatures, and lining thickness for the optimization process.

Table 3
Refractory materials thermal conductivities data

Designation	Refractory material	Thermal conductivities, k (W/(m·K))
A	62% high alumina, Al_2O_3	2
B	carbon composite bricks	12
C	silicon carbide, SiC	120
D	graphite	135

Table 4
Experimental blast furnace data

No.	Description	Value
1	daily furnace production capacity (THM/day)	3000
2	ambient temperature (°C)	28°C (301 K)
3	refractory/shell interface temperature (°C)(K)	45°C (318 K)
4	hearth temperature (°C)(K)	1800°C (2073 K)
5	hearth area (m²)	3.5–6.5
6	hearth height (m)	4
7	hearth diameter (m)	9
8	refractory materials used	high alumina bricks, Al_2O_3(62%), carbon composite bricks, silicon carbide, SiC and graphite
9	constant refractory lining thickness (m)	0.2
10	blast furnace working volume (m³)	1339
11	number of tapholes	2
12	number of tuyeres	2
13	total weight (tons)	9000

This work utilizes four different refractory lining materials, namely 62% high alumina (Al_2O_3), carbon composite bricks, silicon carbide (SiC) and graphite (labeled A, B, C and D), to investigate their roles in furnace optimization through heat interactions within hearth walls.

The lining thickness will be varied for each refractory material to illustrate the effect of an increased thickness on blast furnace productivity and the overall effect comparing each material listed. The same variation process will be applied to the hearth's interior temperatures.

Refractory lining materials will be considered individually to ascertain their heat handling characteristics and this will act as an indication as to the best material when considering the methods of optimization within the hearth region. Figure 7 shows the section of the experimental hearth zone and the various parts.
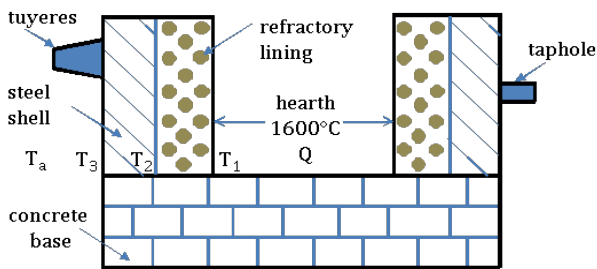

Fig. 7. A section of the hearth region under analysis

3. RESULTS AND DISCUSSION

3.1. Effect of Hearth Refractory Materials

Figures 8 and 9 confer on graphite the property of higher thermal load losses comparable to alumina, silicon carbide and carbon composite at hearth temperature of 1800°C. On the basis of the optimal approach (Figs. 10 and 11), the optimal parameters for the refractory are as specified.

Alumina
Referring to Figure 10, at the optimal level of delivery, the thermal heat load is specified as 100 kW at 1600°C hearth temperature and 3.5 m² surface area. The value of the shell thickness is 68 mm and the lining thickness variation is within the limit of 0.20 m to 0.35 m.

Carbon composite bricks
The thermal heat load is 39 kW, shell thickness is measurable as 70 mm to 74 mm and the lining thickness within the limit of 0.20 m to 0.35 mm.

Silicon carbide
Optimally thermal load losses measured as 2200 kW, shell and lining thicknesses being 100 mm and 0.285 m, respectively.

Graphite
Graphite refractory exhibited the highest thermal load losses, with the numerical value fixed at 5450 kW, shell thickness confirmed as 104 mm and the lining thickness being 0.287 mm.

At hearth operating temperature of 1800°C and surface area 6.5 m², the same trend was observed but with differences in the numerical values of the governing optimal parameter.
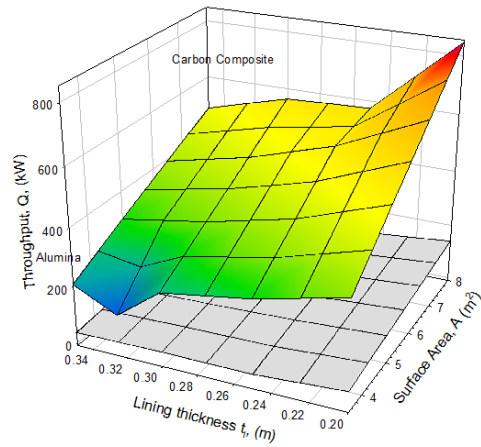

Fig. 8. Hearth throughput variation with lining thickness and surface area for alumina (gray) and carbon composite (colored) at 1800°C
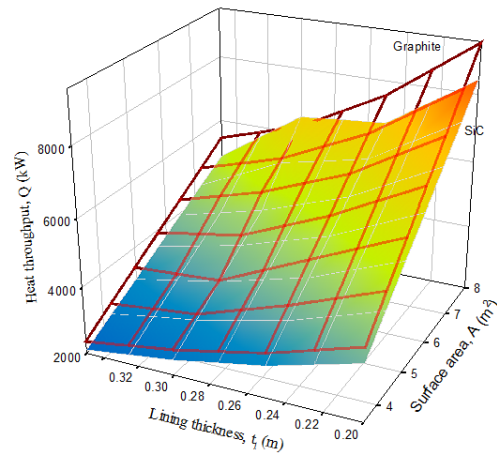

Fig. 9. Hearth throughput variation with lining thickness and surface area for graphite (red gridline) and silicon carbide (colored) at 1800°C
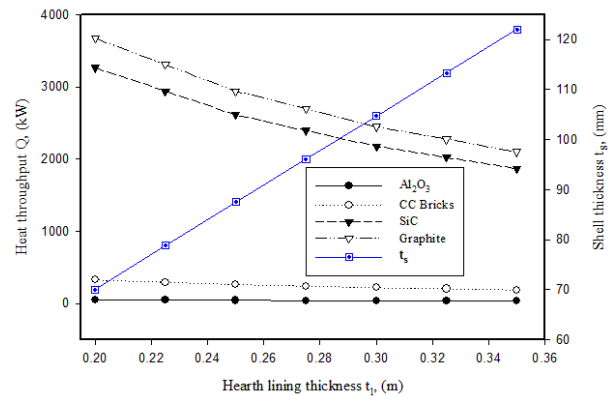

Fig. 10. Heat throughput Q and shell thickness t_s variation with lining thickness t_l for different refractory materials at constant surface area A = 3.5 m², T = 1600°C
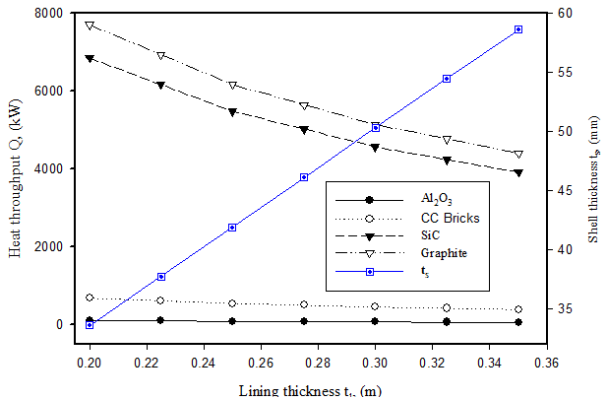
Fig. 11. Heat throughput Q and shell thickness t_s variation with lining thickness t_l for different refractory materials at constant surface area $A = 6.5$ m², $T = 1800$°C

3.2. Effect of Hearth Lining Thickness

From Figures 8 and 9, it was observed that the thinner the hearth refractory lining thickness, the greater the thermal load losses from the system. To this effect, there is ever increasing attention to conserve heat in the hearth region of the blast furnace. This is to ensure excellent fluidity of the molten metal, for smooth and continuous production of the blast furnace; hence, the need for the optimization of refractory thickness in the hearth region.

3.3. Effect of Temperature on Shell Thickness and Throughput

For all the refractories (Figs. 12–14), shell thickness and lining thickness obey direct order but the reverse order to hearth temperature. The relationship of the shell and lining thickness to surface area of the hearth is of the inverse type. Subject to all observable conditions, the shell thicknesses at 1600°C is greater than that at 1800°C. Hence the lower the hearth operating temperature, the thicker the shell thickness, although the conduction heat load losses is higher at higher hearth operating temperature. Saving in terms shell material should be juxtaposed with the thermal load losses in the hearth region to build an efficient blast furnace for iron ore refinement.

It is also worth noting that at constant lining thickness of 0.2 m for a different refractory, conduction heat load increases with increasing thermal conductivities of the refractory materials, while the shell thickness remains relatively constant at 0.0701 m. This is an indication that a refractory with low thermal conductivity will lend itself to excessive heat conservation in the hearth region. Problems of wear, erosion and crack development and propagation and ultimate reduction in the campaign life of blast furnace are undesirable effects. For the variable lining thickness of each refractory, the same trend was observed but with distinct variability in the shell thickness. For 0.2 m to 0.35 m variability in lining, the shell thickness variation is the order of 0.0701 m to 0.122 m at 1600°C (1873 K) temperature.
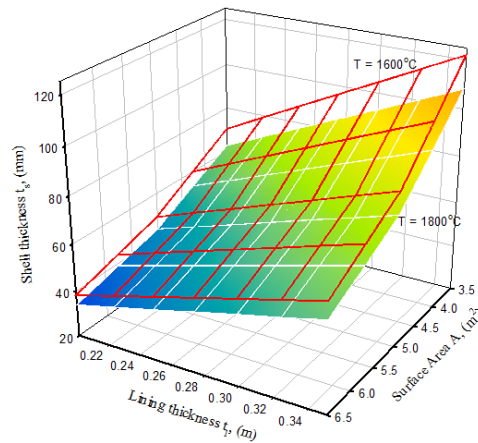

Fig. 12. Effect of temperature on hearth shell thickness t_s variation with lining thickness t_l and surface area A
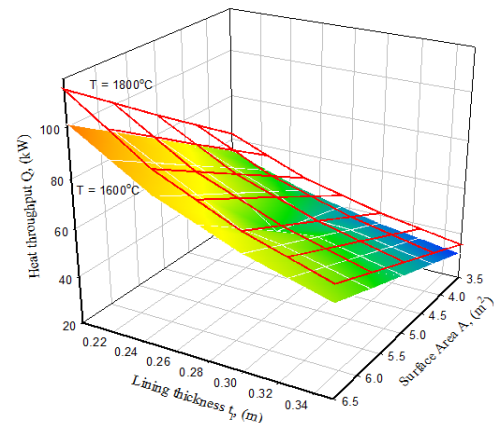

Fig. 13. Effect of temperature on heat throughput variation with hearth lining thickness and surface area of alumina refractory
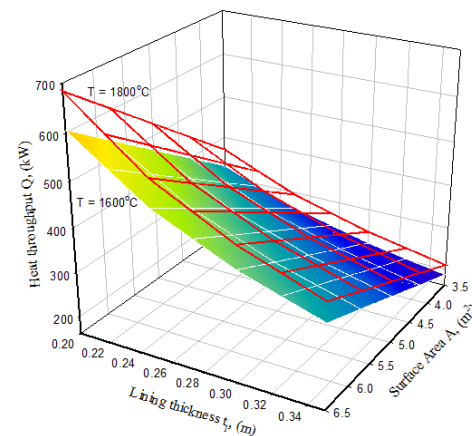

Fig. 14. Effect of temperature on heat throughput variation with hearth lining thickness and surface area of carbon composite bricks refractory

3.4. Effect of Heart Surface Area

Irrespective of the nature and type of refractories (Fig. 15), variation in shell thickness and lining thickness is in direct order while in the reverse manner to the surface area.

Hence, the surface area is in inverse order, an indication of lower thermal load losses with increasing numerical order of shell thickness and refractory thickness.
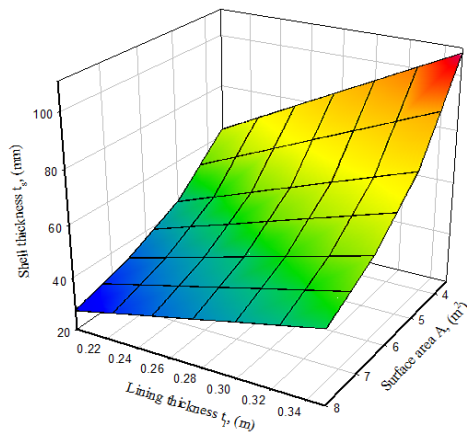
Fig. 15. Hearth shell thickness variation with lining thickness and surface area for all refractory materials at 1800°C

4. CONCLUSION

The heat load consideration in the hearth region of the blast furnace and cooling system is of utmost importance since the wear reactions depend on the lining temperatures. This is all the more so as higher heat conductivity is a superior property in these regions of the blast furnace for three basic reasons:

- the lowering of the refractory hot face temperature to minimize chemical as well as mechanical wear,
- the resistance to temperature shocks is increased,
- the probability of forming a stable skull on the hot face is higher.

REFERENCES

[1] Biswas A.K. (1981). *Principles of blast furnace ironmaking*. Cootha: Brisbane, Australia.

[2] Hebel R., Steiger R. & Streuber C. (1994). Advanced materials for the blast furnace lining in regard to long service life, reasonable cost and theoretical qualification. *Proceedings of 53rd Iron Making Conference, Chicago, March 20–23, AIME – Iron and Steel Society, USA*, 397–406.

[3] Briggs T.A. & Uzoma S.M. (2019). Heat load analysis for optimal use of cupula furnace in iron castings and steel manufacturing. *European Journal of Mechanical Engineering Research*, 6(1), 32–43.

[4] Leimalm U. (2010). Interaction between Pellet Properties and Blast Furnace Operation. Luleå University of Technology, Luleå [Doctoral Thesis].

[5] Dutta S.K. & Chokshi Y.B. (2020). *Blast Furnance Process*. In: Dutta S.K. & Chokshi Y.B., *Basic concepts of Iron and steel making*, Springer, 51–68.

[6] Kumar D. (2015). Optimization of blast furnace parameters using artificial neural network. National Institute of Technology Rourkela-India [Masters Thesis].

[7] Lamont P.H. (1996). Synthetic carbon and graphite – a modern material for the future. *Furnace and Refractory Engineer*, Autumn, 7–11.

[8] Modigell M., Traebert A., Monheim P., Petersen S. & Pickartz U. (2001). A new tool for process modelling of metallurgical processes. *Computers and Chemical Engineering*, 25(4–6), 723–727. Doi: https://doi.org/10.1016/S0098-1354(01)00647-0.

[9] Bhagat P.K. (2015). Optimization of refractory lining used in blast furnace. National Institute of Technology Rourkela-India [Masters Thesis].

[10] Holman J.P. (1983) *Heat transfer*. Fifth Edition. McGraw-Hill International Book Company: New York.

[11] Gdula S.J., Białecki R., Kurpisz K., Nowak A. & Sucheta A. (1985). Mathematical model of steady state heat transfer in the blast furnace hearth and bottom. *Transactions ISIJ*, 25, 380–385.

APPENDIX

Computer Simulation Subroutine

```
% CONDUCTION HEAT LOAD ANALYSIS, OPTIMAL REFRACTORY THICKNESS, DXr AND
% SHELL THICKNESS, DXs FOR THE BLAST FURNACE
% AMBIENT TEMPERATURE, Ta (K)
   Ta=301;
% FURNACE CENTER TEMPERATURE, T1 (K)
   T1=1873;
% TEMPERATURE AT REFRACTORY/SHELL INTERFACE, T2 (K)
    T2=318;
   disp( 'Kgra')
% THERMAL CONDUCTIVITY OF 62% ALUMINA REFRACTORY, Kal (W/mK)
%    Kal=2;
% THERMAL CONDUCTIVITY OF CARBON COMPOSITE BRICK, Kccb (W/mK)
     Kccb=12;
% THERMAL CONDUCTIVITY OF SILICON CARBIDE REFRACTORY, Ksc (W/mK)
     Ksc=120;
% THERMAL CONDUCTIVITY OF GRAPHITE REFRACTORY, Kgra (W/mK)
     Kgra=135;
%  HEARTH RADIUS, r3 (m)
     r3=4.5;
%  HEARTH LENGHT, L (m)
     L=4;
     for  A=3.5:1.5:12.5
        disp('A-Hearth Surface Area')
         fprintf('%20.4f\n',A)
%  HERATH SURFACE AREA, A(m2)
%     A=3.5;
% LET DXr (m) REPRESENTS THE THICKNESS OF THE REFRACTORY LINING
     for DXr=0.2:0.05:0.35
         disp( 'DXr--Refractory Thickness')
         fprintf('%20.4f\n',DXr)
%  Q--is the conduction heat load in Watts
     Q=(Kgra*A*(T1-T2))/DXr;
     q1=(2*pi*Kgra*L*(T2-Ta))/Q;
     disp( 'q1')
     q2=exp(q1);
     disp( 'q2')
     fprintf('%20.10f\n',q1,q2)
     r2=r3/q2;
%  SHELL THICKNESS, DXs (m)
     DXs=r3-r2;
     disp( 'DXs--Shell Thickness')
     fprintf('%20.4f\n',DXs)
     disp('Q-Conduction Heat Load (Watts)')
     fprintf('%20.4f\n',Q)
   end
   end
```